ISBN: 978-3-95450-184-7 doi:10.18429/JACoW-IPAC2018-TUXGBF2

HIGHER-ORDER-MODE EFFECTS IN SUPERCONDUCTING RF CAVITIES ON ELECTRON-BEAM QUALITY*

A. H. Lumpkin[1†], D. Edstrom, N.Eddy, O. Napoly[2], P. Prieto, J. Ruan, R. Thurman-Keup,
Fermi National Accelerator Laboratory, Batavia, IL 60510 USA
B. Carlsten, K. Bishofberger [1]LANL, Los Alamos, NM, 87545 USA
[2]CEA-Saclay, Gif-sur-Yvette, France

Abstract

We report the direct observations of the correlation of higher order modes (HOMs) generated by off-axis electron beam steering in TESLA-type SCRF cavities and sub-macropulse beam centroid shifts (with the potential concomitant effect on averaged beam size and emittance). The experiments were performed at the Fermilab Accelerator Science and Technology (FAST) facility using its unique configuration of a PC rf gun injecting beam into two separated 9-cell cavities in series with corrector magnets and beam position monitors (BPMs) located before, between, and after them. The ~100-kHz oscillations with up to 300-µm amplitudes at downstream locations were observed in a 3-MHz micropulse repetition rate beam with charges of 100, 300, 500, and 1000 pC/b, although the effects were much reduced at 100 pC/b.

INTRODUCTION

The interest in beam quality preservation through accelerator structures [1] continues as the community constructs larger facilities and pushes toward brighter beams. Several major facilities depend on the superconducting RF TESLA-type L-band accelerator modules [2,3] including the FLASH free-electron laser (FEL) [4], the European XFEL [5], the under-construction LCLS-II XFEL [6], the proposed MaRIE XFEL at Los Alamos [7], and the International Linear Collider (ILC) under consideration in Japan [8]. A recent study at FLASH using one specific TE_{111} HOM showed that the root mean squared (rms) relative alignments were about 342 µm for the 40 cavities in the 5 cryomodules with some close to 600 µm off axis [9]. The assessment of the effects on beam quality of such implementations warrants further study as higher brightness electron beams are sought and achieved.

We have explored the effects of beam-induced higher order modes on the pulse train at the Fermilab Accelerator Science and Technology (FAST) facility which is based on TESLA-type cavities [10]. Direct measurement of the transverse magnetic dipole modes' power in the first two passbands as outcoupled were tracked and correlated with the beam motion as a complement of studies on cavity misalignments [9,11-15]. Initial calculations reproduced a key feature of the phenomena. In principle, these results may be scaled to cryomodule configurations of major accelerator facilities.

* Work at Fermilab supported by Fermi Research Alliance, LLC under Contract No. DE-AC02- 07CH11359 with the United States Department of Energy.
*** Work at Los Alamos supported by the US Department of Energy through the LANL/LDRD Program
† lumpkin@fnal.gov

EXPERIMENTAL SETUP/TECHNIQUES

The FAST linac [15] is based on an L-band rf photocathode (PC) gun which generates and accelerates an electron beam with a 3-MHz micropulse (or bunch (b)) repetition rate up to 5 MeV. The gun's Cs_2Te photocathode is irradiated by the UV component of the drive laser system [16]. The two HOM-instrumented SCRF capture cavities denoted CC1 and CC2 follow [15]. These accelerate the electron beam up to 50 MeV for transport through the remaining low energy beamline as shown in Fig. 1. Under nominal low-energy operation conditions, the magnet at beamline location 122 bends the beam downward into the low energy absorber to provide a final beam energy measurement. This and other nominal beam parameters for these studies are summarized in Table 1.

Table 1: Beam Parameters at the FAST Linac

Beam Parameter	Units	Value
Micropulse Charge	pC	100-1000
Micropulse Rep. rate	MHz	1,3
Beam sizes (sigma)	µm	100-1200
Emittance Norm.	mm mrad	1-5
Bunch length	ps	4-8
Total Energy	MeV	33

For the purposes of these studies, the final beam energy was kept constant at 33 MeV with a range of micropulse charges utilized as indicated. The basic diagnostics for the HOM studies include the rf BPMs (denoted as B1xx) located before, between, and after the two cavities as shown in Fig. 1 as well as ten BPMs before the low energy spectrometer dipole. These are supplemented by the imaging screens inserted into beam line vacuum crosses (Xyyy) denoted at X107, X111, X121, and X124. The HOM couplers

9th International Particle Accelerator Conference IPAC2018, Vancouver, BC, Canada JACoW Publishing
ISBN: 978-3-95450-184-7 doi:10.18429/JACoW-IPAC2018-TUXGBF2

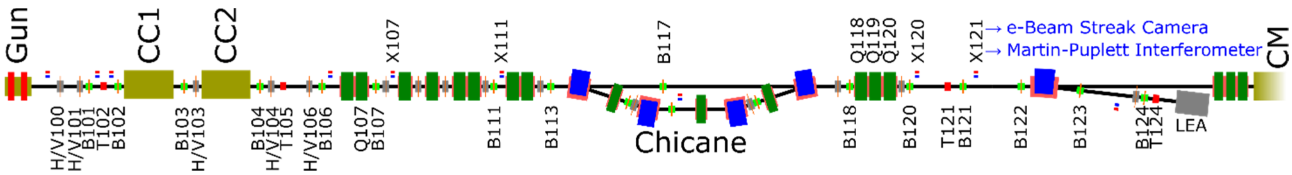

Figure 1: Schematic of the FAST low-energy beamline showing the PC rf gun, capture cavities CC1 and CC2, horizontal and vertical correctors, rf BPM locations, key imaging stations, and the beginning of the cryomodule (CM).

are located at the upstream and downstream ends of each SCRF cavity [9], and these signals are processed by the HOM detector circuits with the output provided online through ACNET, the Fermilab accelerator controls network. Recent upgrades included optimizing the HOM detectors' bandpass filters to target the two dipole passbands from 1.6-1.9 GHz, converting the rf BPM electronics to support bunch-by-bunch measurements with reduced noise [17,18], and installation of an imaging screen and W plate with multi-slits at X107 to enable transverse emittance measurements. At this latter location, the beam size of 1 mm used to illuminate multiple slits limited sensitivity to the beam oscillations in averaged beam images, but they were clearly seen in the time-resolved rf BPMs. A commissioned cryomodule with 250-MeV acceleration capability [19] is located downstream, but it was not involved in these initial studies.

EXPERIMENTAL RESULTS

The experimental results include HOM detector data from CC1 and CC2, the bunch-by-bunch beam-position data, and the preliminary beam size measurements correlated with the upstream correctors and micropulse charges.

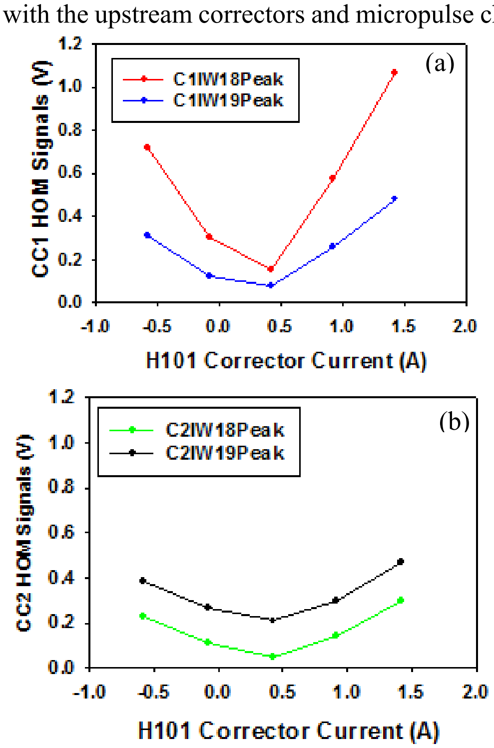

Figure 2: Examples of the H101 corrector current scans that identify HOM detector minima for 500 pC/b in both (a) CC1 and (b) CC2.

HOM-Related Results

In Fig. 2 we show examples of the dependence of the four HOM detector signals on the H101 corrector settings. In this case the V101 dipole corrector was set to a nominal value of 0.0A, and the H/V103 correctors were set to minimize the CC2 HOM signals as well. From such data, the H101=0.42 A setting was chosen in the operations setup since all four HOM detector signals are close to their relative minimum value. The corrector scans are done with a range of ±1 A from these reference values.

rf BPM-Related Results

The most striking effects were seen in the bunch-by-bunch rf BPM data. In Fig. 3 we display the time dependence of the bunch centroid position as detected at B120 in a 500-b macropulse with vertical corrector V101=1 A. A 100-kHz centroid oscillation is noted at a micropulse charge of 500 pC. This amplitude is observed to dampen in the first 200 b, although the slew in position continues to the end of the train. The macropulse-averaged centroid position has been determined and subtracted prior to display.

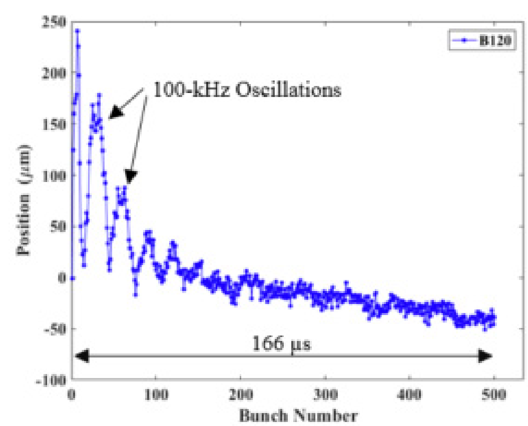

Figure 3: Vertical centroid oscillations shown at rf BPM location B120 for 500 b, 500 pC/b, and V101=+1A. The 100-kHz oscillation decays noticeably in the first 200 b, and a centroid slew continues to the end of the macropulse.

We then focused on the oscillations in a 50-b train as shown in Fig. 4a. The oscillation basically has a period of 30 b at 3 MHz (or 100 kHz) in B122. The oscillation amplitude was evaluated by fitting a parabola over the peaks near bunch 15 and 30 to determine the peak-to-peak amplitude. In Fig. 4b we show the results of such analysis for

ISBN: 978-3-95450-184-7 doi:10.18429/JACoW-IPAC2018-TUXGBF2

the 10 BPM locations after CC2. We also show the amplitude appears unchanged with corrector setting at B103V, implying the HOM kick was in CC2. In Fig. 5 we show a calculation of the kick angle during the macropulse due to the HOM mode 14 in passband 2 (Nomenclature of [20]).

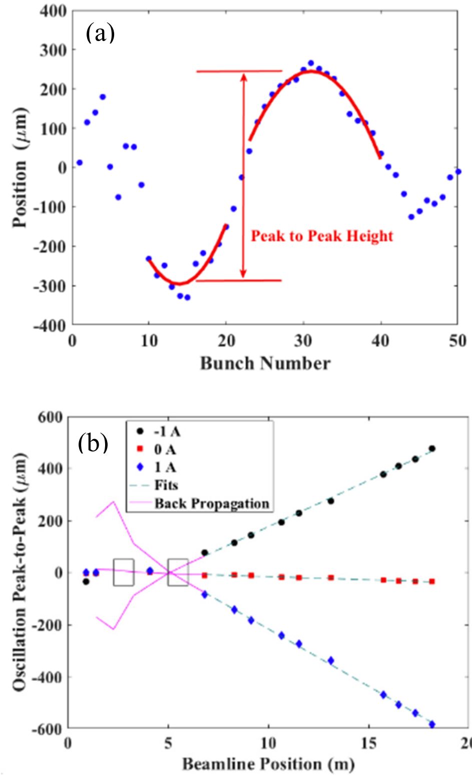

Figure 4 : Observed beam centroid oscillations during the V101 scan. (a) the example from B122V illustrating the oscillation amplitude assessment technique and (b) the plot of the amplitudes for the 3 BPMs upstream of CC2 and the 10 BPM locations after CC2.

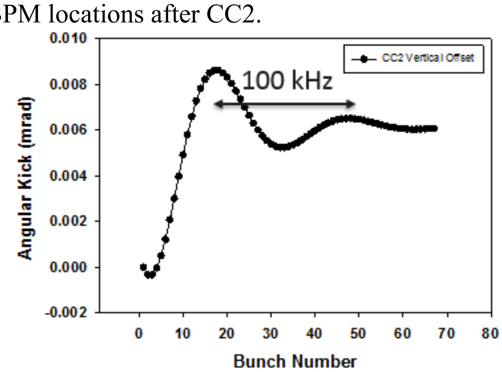

Figure 5: Calculated kick angle vs. bunch number for a 5-mm vertical offset in CC2 for Mode 14 with vertical polarization. The mode frequency and beam harmonic have a 100-kHz difference, which gives this resonant kick.

X107-Related Results

The rf BPM data indicated a centroid oscillation of ±100 μm at the location just before the X107 screen for a V101 corrector steering of +1A and 500 pC/b. Since the initial beam size was 1,174 μm (132 pixels x 8.9 μm/pixel) at X107, the averaged beam size effects would be small. However, a centroid slew was also indicated in the B106 data, and such a slew during the macropulse may also contribute to a broadened average beam size. We observed an averaged maximal effect of ~6%, or 72 μm, in Fig. 6a which was correlated with the maximal HOM sum signal strength as shown in Fig. 6b. In addition, effects on the beam divergence would be expected since angular kicks were generated.

The vertical multislits were then inserted at X107 [21], and then the slit images were viewed 1.54 m downstream at X111 as shown in Fig. 7a. The widths of the slit images provided the divergence information compared to the fixed rms slit-width contribution of 11.5 μm. For this V101=0.5 A case, the average observed projected slit profile width was 8.5±0.5 pixels or 76 μm as shown in Fig 7b. The averaged horizontal divergence would thus be 50 μrad, or 49 μrad corrected for the slit finite size. In the case of vertical divergence, the orthogonal set of slits was inserted and images evaluated. Further studies are needed on this aspect and on the feasibility of supporting the HOM studies.

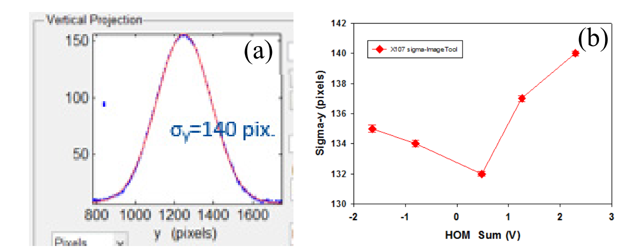

Figure 6: Results of imaging at X107: a) the Gaussian fit to the projected y profile for largest HOM sum, and b) the projected profile fitted sigma values vs. HOM sum values in the V101 scan. The sum signs were from the corrector values for plotting purposes to display the correlation.

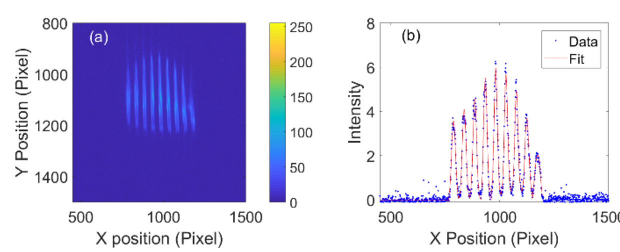

Figure 7: a) Example of X107 multi-slit image as viewed 1.54 m downstream at X111. b) projected profiles of the slit images (blue) with Gaussian fits indicated (red).

SUMMARY AND CONCLUSIONS

In summary, we have observed clear correlations of beam mis-steering into CC1 and CC2, HOM detector signal strength, and sub-macropulse beam centroid oscillation amplitudes at the few 100-μm regime or more depending on the drift distance. The beam-size effects are relatively minor for our emittance ranges and optics, but we anticipate that such effects would be an issue for ultra-low emittance beams [22]. We next plan to apply the techniques to the full cryomodule downstream of the capture cavities and evaluate those effects. The relevance of these unique data to major facilities will then be re-evaluated.

ISBN: 978-3-95450-184-7 doi:10.18429/JACoW-IPAC2018-TUXGBF2

ACKNOWLEDGMENTS

The authors acknowledge the technical support of J. Santucci, D. Crawford, and B. Fellenz; the project support of J. Liebfritz; the mechanical support of C. Baffes; the lattice assistance of S. Romanov; the cold cavity HOM measurements of A. Lunin and T. Khabiboulline of the Technical Division, the SCRF support of E. Harms; discussions with S. Yakovlev and Y. Shin; as well as the discussions with and/or support of A.Valishev, D. Broemmelsiek, V. Shiltsev, and S. Nagaitsev of the Accelerator Division at Fermilab. The Fermilab authors acknowledge the support of Fermi Research Alliance, LLC under Contract No. DE-AC02- 07CH11359 with the United States Department of Energy. The Los Alamos authors gratefully acknowledge the support of the US Department of Energy through the LANL/LDRD Program for this work.

REFERENCES

[1] W.K.H. Panofsky and M. Bander, *Rev. Sci. Instrum*., vol 39, p. 206, 1968.

[2] TESLA-Technical Design Report, DESY-TESLA-2001-23, edited by R. Brinkman et al., 2001.

[3] S. Fartoukh *et al*., "Evidence for a Strongly Coupled Dipole Mode with Insufficient Damping in TTF First Accelerating Module", DAPNIA/SEA/99-18 and *Proc. PAC'99*, vol. 2, p. 922, 1999.

[4] J. Rossbach, *NIM* A475, p. 13, 2001: K. Honkavaara, "Status of the FLASH FEL User Facility at DESY", *Proc. FEL'17*, MOD02, Santa Fe, NM, **www.JACoW.org**

[5] H. Weise, "Commissioning and First Lasing of the European XFEL", in *Proc. FEL'17*, paper MOC03, Santa Fe, NM, **www.JACoW.org**

[6] P. Emma, "Status of the LCLS-II FEL Project at SLAC", in *Proc. FEL'17*, paper MOD01, Santa Fe, NM, **www.JACoW.org**

[7] R.L. Sheffield, "Matter-Radiation Interactions in Extremes (MaRIE) Project Overview", in *Proc. FEL'17*, paper MOD06, Santa Fe, NM, **www.JACoW.org**

[8] "Conclusions on the 250 GeV ILC as a Higgs Factory proposed by the Japanese HEP community", ICFA, November 8, 2017.

[9] Thorsten Hellert, Nicoleta Baboi, and Liangliang Shi, "Higher Order Mode Based Cavity Misalignment Measurements at the Free- electron Laser FLASH", *Phys. Rev. Accel. Beams*, vol 20, p. 090701, 2017.

[10] Sergey Antipov *et al*., JINST. **12** T03002, (2017).

[11] N. Baboi, G.Kreps, M.Wendt, G.Devanz, O. Napoly, R.G. Paparella, "Preliminary Study on HOM-based Beam Alignment in the TESLA Test Facility", in *Proc. LINAC'04*, paper MOP36, Lubeck, Germany.

[12] Ch. Magne *et al*., "Measurement with Beam of the Deflecting Higher Order Modes in the TTF Superconducting Cavities", in *Proc. PAC'01*, Chicago IL, p. 3771. **www.JACoW.org**

[13] Stephen Malloy *et al*., *Phys. Rev. ST Accel*. Beams, vol. 9, p. 112802, 2006.

[14] Stephen Malloy *et al*., *Meas. Sci. Technology*, vol. 18, pp. 2314-2319, (2007.

[15] D. Edstrom *et al*., "50-MeV Run of the IOTA/FAST Electron Accelerator", in *Proc. NAPAC'16*, paper TUPOA19, Chicago, IL, **www.JACoW.org**

[16] J. Ruan *et al*., *in Proc. IPAC'13*, paper WEPME057, **www.JACoW.org**

[17] N. Eddy *et al*., "High Resolution BPM Upgrade for the ATF Damping Ring at KEK", DIPAC 2011, Hamburg,DE.

[18] N. Patel *et al*., "Beam Position Monitoring System for the PIP-II Injector Test Accelerator", in *Proc. NAPAC'16*, paper TUPOA29, Chicago, IL, **www.JACoW.org**

[19] A. Romanov *et al*., "Commissioning and Operation of FAST Electron Linac at Fermilab", presented at IAPC'18, paper THPMF024, this conference.

[20] Rainer Wanzenberg, TESLA Report 2001-33; and "HOMs in the TESLA 9-cell Cavity", *SPL HOM Workshop*, CERN, June 25-26, 2009.

[21] J. Ruan *et al*., "Emittance Study at the FAST Facility", presented at IAPC'18, paper THPMF025, this conference.

[22] A.H. Lumpkin *et al*., "Sub-Macropulse Electron-beam Dynamics Correlated with Higher-Order Modes in TESLA-type Superconducting RF Cavities", accepted in *Phys. Rev. Accelerators and Beams*, April 2018.